Обзор ArXiv/astro-ph, 15-22 февраля 2023

От Сильченко О.К.

ArXiv: 2302.08405

The X-ray invisible Universe. A look into the halos undetected by eROSITA

P. Popesso,[1]⋆ A. Biviano,[2,3] E. Bulbul,[4] A. Merloni,[4] J. Comparat,[4] N. Clerc, Z. Igo,[4] A. Liu,[4] S. Driver,[6] M. Salvato,[4] M. Brusa,[7] Y.E. Bahar,[4] N. Malavasi,[8] V. Ghirardini,[4] A. Robotham,[5] J. Liske,[9] S. Grandis[8]

[1]*European Southern Observatory, Karl Schwarzschildstrasse 2, 85748, Garching bei München, Germany*
[2]*INAF-Osservatorio Astronomico di Trieste, via G.B. Tiepolo, 11 - Trieste (Italy) I-34143*
[3]*IFPU Institute for Fundamental Physics of the Universe, via Beirut, 2 - Trieste (Italy) I-34014*
[4]*Max Planck Institut für extraterrestrische Physik (MPE), Postfach 1312, D85741, Garching, Germany*
[5]*IRAP-Roche, 9, avenue du Colonel Roche BP 44346 31028 Toulouse Cedex 4*
[6] *International Centre for Radio Astronomy Research (ICRAR), University of Western Australia, Crawley, WA 6009, Australia*
[7] *Dipartimento di Fisica e Astronomia, Universita' di Bologna, Via Gobetti 93/2, 40129, Bologna, Italy*
[8] *Universitaïs-Sternwarte Muñchen / Observatorium Wendelstein Scheinerstraße 1, D-81679 München, Deutschland*
[9]*Universität Hamburg, Department of Physics, Hamburg Observatory, Gojenbergsweg 112, 21029 Hamburg*

Accepted XXX. Received YYY; in original form ZZZ

ABSTRACT

The paper presents the analysis of GAMA spectroscopic groups and clusters detected and undetected in the SRG/eROSITA X-ray map of the eFEDS (eROSITA Final Equatorial Depth Survey) area, in the halo mass range $10^{13} - 5x10^{14}$ $M_{\odot}$ and at $z < 0.2$. We compare the X-ray surface brightness profiles of the eROSITA detected groups with the mean stacked profile of the undetected low-mass halos. Overall, we find that the undetected groups exhibit less concentrated X-ray surface brightness, dark matter, and galaxy distributions with respect to the X-ray detected halos. Consistently with the low mass concentration, the magnitude gap indicates that these are younger systems. The later assembly time is confirmed by the bluer average color of the BCG and of the galaxy population with respect to the detected systems. They reside with a higher probability in filaments while X-ray detected low-mass halos favor the nodes of the Cosmic Web. Because of the suppressed X-ray central emission, the undetected systems tend to be X-ray under-luminous at fixed halo mass, and to lie below the $L_X - M_{halo}$ relation. Interestingly, the X-ray detected systems inhabiting the nodes scatter the less around the relation, while those in filaments tend to lie below it.

Группы галактик в обзоре GAMA

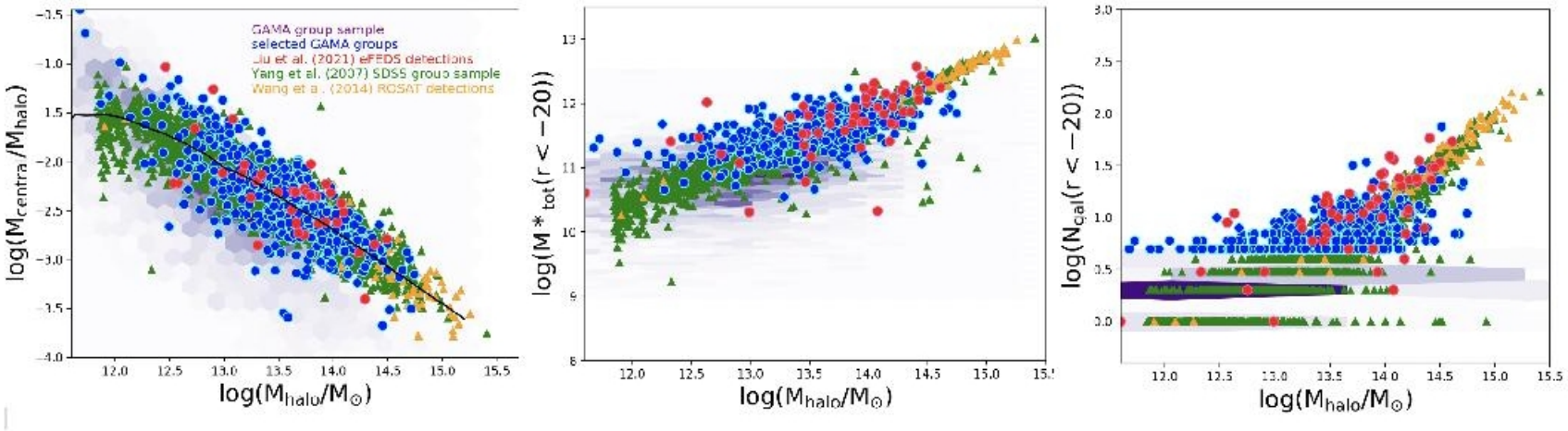

Figure 1. Optical properties of the GAMA undetected and the eFEDS detected systems. We compare the two samples with the SDSS group sample of Yang et al. (2007) in a similar redshift range and with the sample of Wang et al. (2014), who provide the ROSAT detections of the optically selected groups. **Left panel:** ratio of the central galaxy stellar mass over the halo mass versus the halo mass. We use M_{200} for all samples, by correcting for the different cosmology when needed. The same halo mass is used in all panels. The purple-shaded region indicates the density distribution of all GAMA groups in the diagram. The blue points indicate the GAMA undetected groups considered in this work. The red points indicate the eFEDS-detected systems. The green triangles show the Yang et al. (2007) systems while the orange triangles indicate the subsample with a $SNR > 5$ ROSAT detections in Wang et al. (2014). The same color coding is applied to all panels. **Central panel:** Total stellar mass of the groups versus halo mass based on the GAMA velocity dispersion. The total stellar mass is estimated by considering all system members brighter than $r_{mag} = -20$. **Right panel:** System richness versus halo mass. The richness is estimated as the number of system members brighter than $r_{mag} = -20$.

Еще раз выборка – сравнение с LCDM моделями

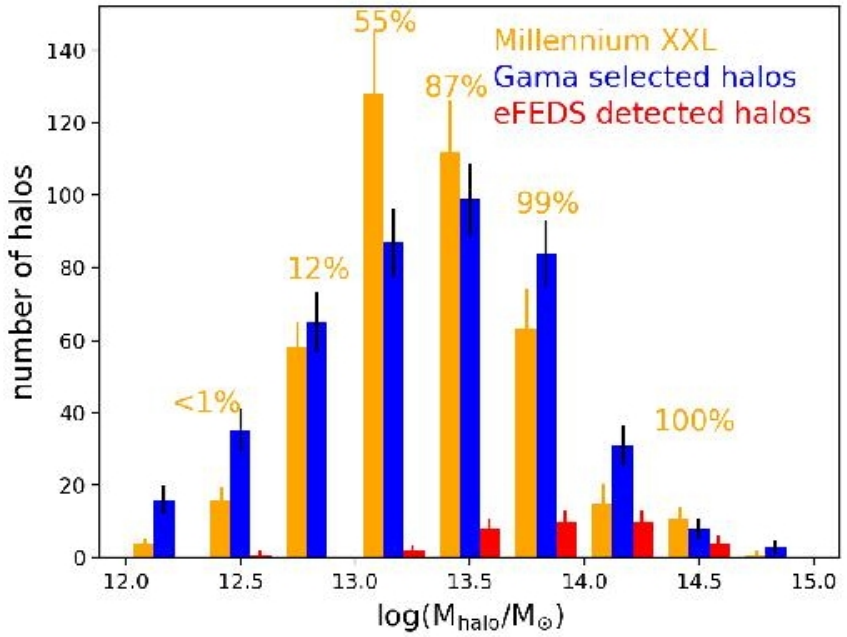

Figure 2. Halo mass distribution in the Millennium XXL sample, averaged over ten volumes as large as the one sampled by the overlap of the eFEDS and GAMA area in the redshift range $0 < z < 0.2$ (orange histogram). The red histogram indicates the X-ray detected eFEDS sample in the overlap region of the GAMA and eFEDS area. The blue histogram shows the optically selected GAMA group sample in the same area. The cut in richness ≥ 5 of galaxy members is applied to all samples for consistency. We also indicate the percentage of halos obtained after the cut in richness with respect to the parent sample in the Millennium XXL sample. Orange, blue, and red histograms are in the same halo mass bins but are displaced along the x-axis for the sake of clarity.

Окончательный размер выборки

The selection procedure described above leads to a sample of 189 systems at $z < 0.2$, with ≥ 5 spectroscopic members, and $M_{200} \geq 10^{13} M_{\odot}$, of which 32 detected in X-ray and 157 undetected. In Fig. 3 we show the comparison between the M_{500} estimates obtained from the X-ray data analysis Liu et al. (2022a, see for details), $M_{500,X}$, that are available for 26 out of the 32 detected systems, and the corresponding estimates obtained from the system velocity dispersion, $M_{500,\sigma}$. Apart from an obvious outlier, the two mass estimates agree very well, with a median ratio $M_{500,X}/M_{500,\sigma} = 0.96$. The outlier in the relation is due to a different redshift assignment of the redMapper algorithm applied by (Klein et al. 2022) and the optical group counterpart in the GAMA group sample.

Радиальные профили рентгена

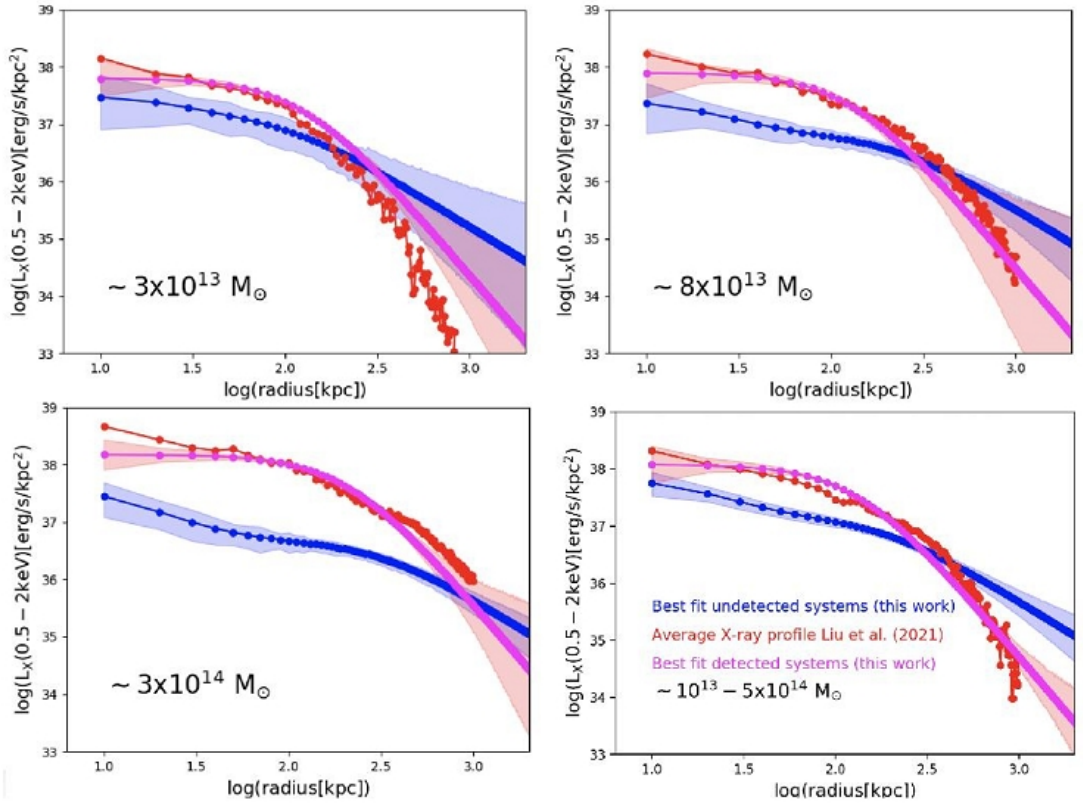

Figure 4. The two upper panels and the bottom left panel show the mean X-ray surface brightness of detected and undetected sources in three bins of halo mass, derived from the GAMA velocity dispersion. The bottom right panel shows the same comparison between the detected sample and a mass-matched sub-sample of the undetected systems over the whole available halo mass range. The blue line shows the best fit of the stacked undetected GAMA systems, while the blue-shaded region shows the error of the corresponding observed mean profile. The magenta line shows the best fit of the stacked detected eFEDS systems, and the corresponding shaded region shows the error of the observed mean profile. For comparison, the connected red points show the mean profile obtained by averaging the X-ray surface brightness profile of Liu et al. (2022a) of the same systems.

Ищем различия между группами detected/undetected в рентгене

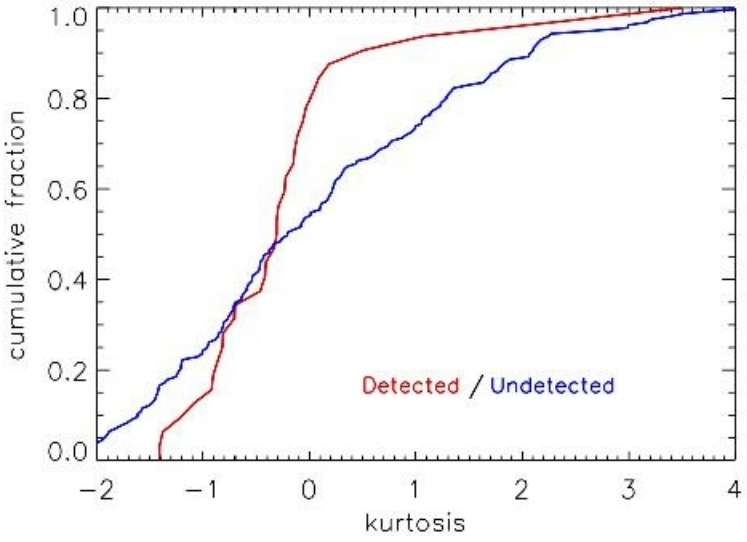

Figure 6. Cumulative distribution of the kurtosis of the velocity distributions of X-ray detected (red) and undetected (blue) groups.

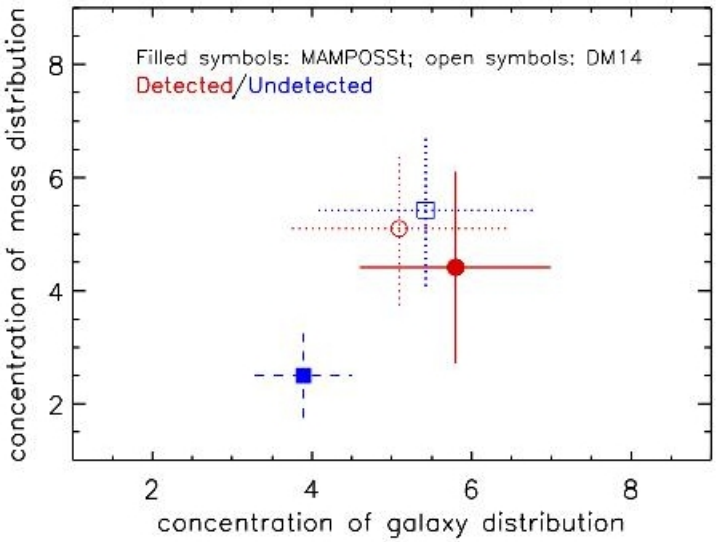

Figure 8. Concentration of the distribution of mass, c_ρ, vs. the concentration of the distribution of group galaxies, c_g for X-ray detected groups (red dot and solid 1-σ error bars), and undetected groups (blue square and dashed 1-σ error bars). Filled symbols indicate the results of the MAMPOSSt analysis. Open symbols and dotted lines indicate predictions from numerical simu-

Ищем различия между группами detected/undetected в рентгене

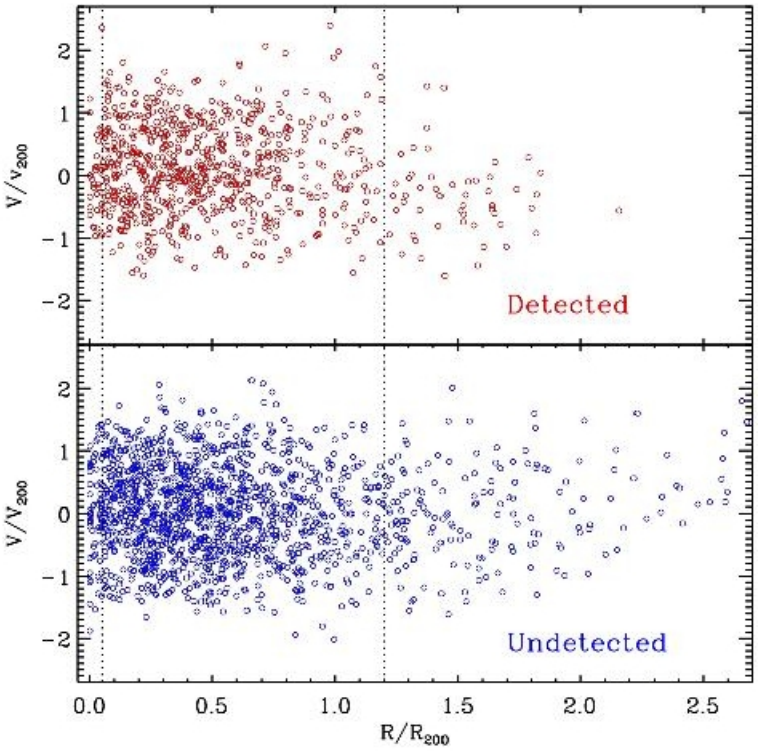

Figure 7. Projected-phase-space distributions of the stacked samples of X-ray detected (top panel) and undetected (bottom panel) groups. The dotted line indicates the radial range used in the MAMPOSSt analysis.

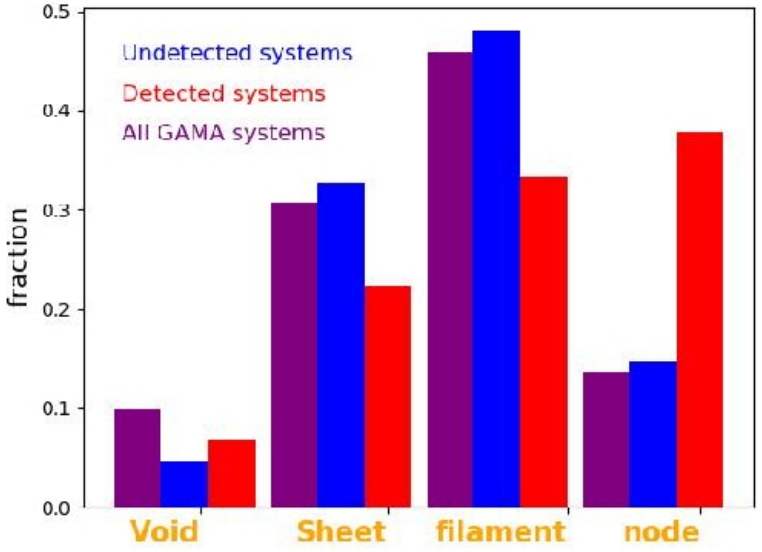

Figure 9. Distribution of the X-ray undetected GAMA (blue histogram), X-ray detected eFEDS (red histogram) and the whole GAMA sample with richness higher than 5 (purple histogram) in the 4 classes of the Cosmic Web at $z < 0.2$ identified in the GAMA spectroscopic sample by Eardley et al. (2015)

… по широкому спектру параметров

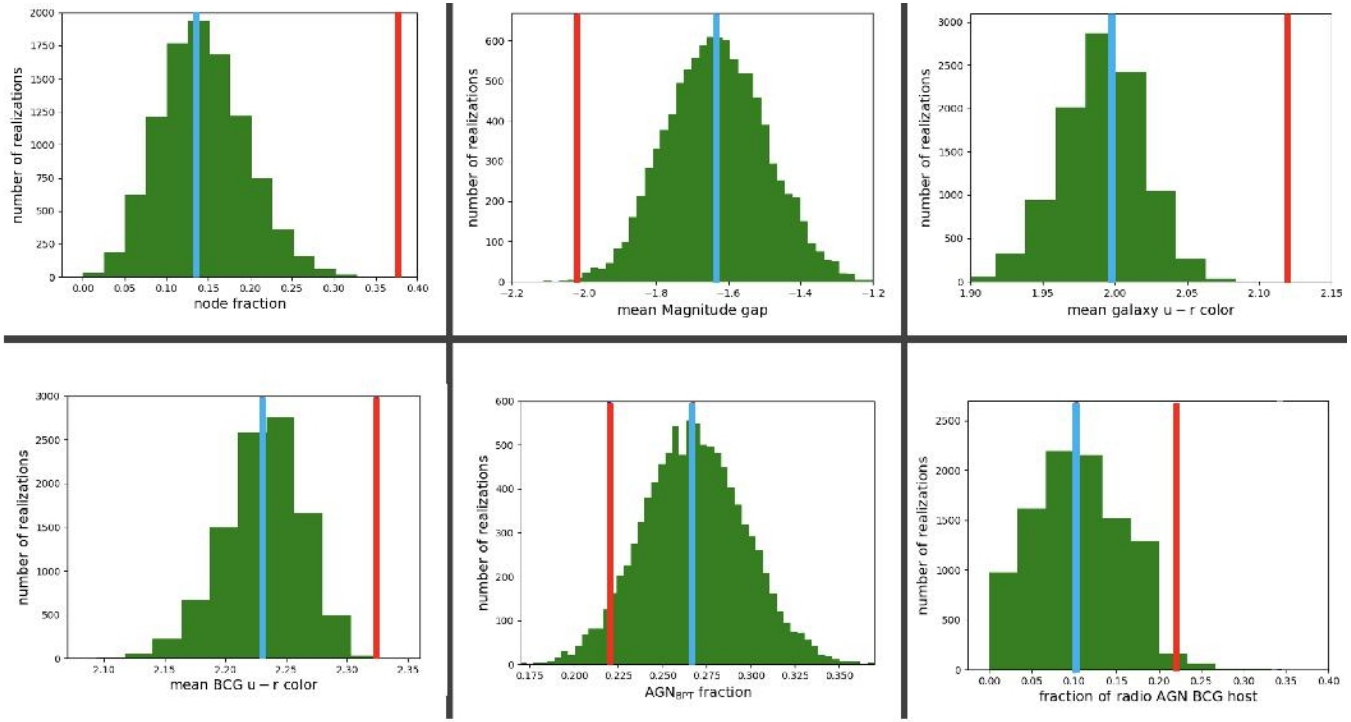

Figure 10. Comparison of the mean properties of the detected systems (red line in all panels) and the mean properties of 10000 halo mass-matched samples randomly extracted from the undetected system sample. Each panel shows the corresponding mean value (cyan line) and the distribution in the 10000 random extractions (green histogram). The upper panels from left to right show the comparison of *i)* the fraction of systems localized in the nodes of the Cosmic web *ii)* the mean magnitude gap between the first and the second brightest galaxies in the r band, and *iii)* the mean $u - r$ rest frame color of the galaxy population per group. The bottom panels from left to right show: *iv)* the mean $u - r$ rest frame color of the BCG, *v)* the mean fraction of optical AGN hosts per group and *vi)* the probability that the BCG host a radio AGN.

Вывод: рентген бывает только у старых групп в узлах крупномасштабной структуры

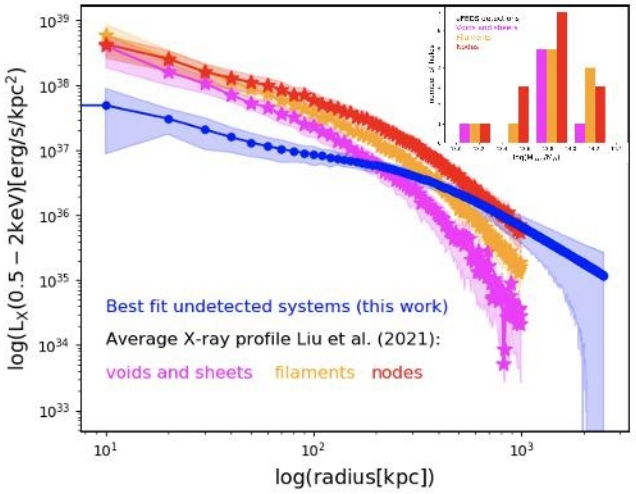

Figure 12. The panel shows the mean X-ray surface brightness of the detected systems provided by Liu et al. (2022a) in three Cosmic Web components: voids and sheets (magenta profile), filaments (orange profile), and nodes (red profiles). The blue line region shows the mean stacked profile of the undetected systems with a similar halo mass distribution as for the detected systems. The shaded regions for all profiles represent the 1σ error retrieved from the bootstrapping analysis. The histogram in the inner panel shows the mass distribution of the detected systems divided by the Cosmic Web component. The histograms are artificially displaced from one another for clarity. The median of the mass distribution is the same for all components.

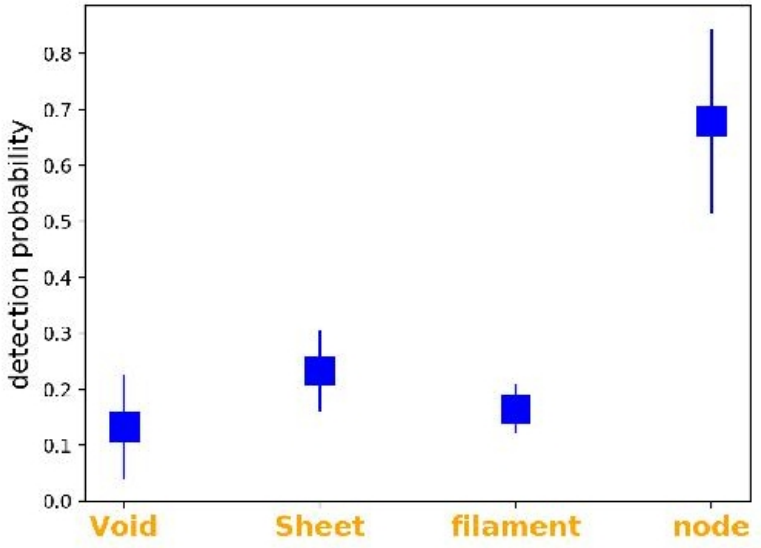

Figure 13. Detection probability of halos above $2\times10^{13}\ M_{\odot}$ per Cosmic Web component in the eROSITA soft band at the eFEDS depth. The probability is estimated as the fraction of eFEDS detection over the number of the underlying halo population per Cosmic Web component, represented by our sub-sample of optically selected GAMA systems.